Optics Communications 391 (2017) 100–105

Contents lists available at ScienceDirect

Optics Communications

journal homepage: www.elsevier.com/locate/optcom

Generation of a sequence of correlated phase screens☆

Parisa Fatheddin[a,b,*], Jonathan Gustafsson[c,d]

[a] Department of Engineering Physics, Center for Directed Energy, Wright-Patterson AFB, Dayton, OH 45433, USA
[b] Oak Ridge Institute for Science and Education, 1299 Bethel Valley Road, Oak Ridge, TN 37380, USA
[c] Department of Mathematics and Statistics, Air Force Institute of Technology, WPAFB, OH 45433, USA
[d] National Research Council, 500 Fifth Street NW, Washington, DC 20001, USA

ARTICLE INFO

Keywords:
Laser propagation
Random media
Phase screens

ABSTRACT

A novel technique is given and implemented to generate correlated phase screens that are used in the study of laser propagation through turbulent atmosphere. The method can generate random fields with nonzero expected values and is applied to simulate equally and arbitrary spaced phase screens. In both cases, it proves to be very computationally efficient.

1. Introduction

Laser propagation through random media has seen extensive investigation. It has many important applications in the improvement of image resolution of telescopes, in industry in welding of metals and in medicine in laser surgery (see for example [1,11,14,20]). One can observe the significance in the precision of directing lasers through random media. To this end, lasers are modeled as electromagnetic waves whose refractive index become altered as they go through a medium as a cause of temperature and density fluctuations in the atmosphere. These alterations in turn change the phase of the waves, which have promoted the idea of dividing the medium into phase screens indicating where the phase changes. The screens can be thought of as two or three dimensional layers or slabs. For more background on laser propagation through random media we recommend [2,11,12,16].

To generate phase screens, many numerical simulation methods have been proposed. The classical approach is the Monte Carlo simulation which creates random arrays of phase values in a grid of sample points that have the same statistics as the turbulence-induced atmospheric phase. Here we will use Fourier filtering method, which is based on the Fast Fourier Transform (FFT) of the process with the requirement that the process be stationary. Similar to our result, Xiao and Voelz [21] also applied the Fast Fourier Transform technique to simulate phase screens. They simulated uncorrelated phase screens to examine the intensity of laser light as it propagates. In addition, Dieker and Mandjes used this simulation approach in [4] to compute the discrete Fourier transform of one dimensional fractional Brownian motion (fBm). Since fBm does not posses the stationary requirement, the stationary property of its increments given as white noise is used instead. For two and three dimensions, [22] gives this method for fBm using the turning band method, which he claims to be faster and more accurate than the Fourier filtering method; however, we find the Fourier filtering method more accessible and easier to implement. Here we provide details to Fourier filtering technique and apply it to generate two and three dimensional phase screens correlated by temperature. Our simulation technique has also been applied to a stationary Gaussian process in [6] and explained in [14]. We extend the results of [6] by not requiring the mean of the Gaussian random field to be zero. Chapter 12 of [15] also uses fast Fourier transform and provides detailed steps for the simulation of important types of spatial processes such as Gaussian and Markov random fields, point processes, spatial Wiener processes and Levy fields. Here we have a similar situation since the temperature at each point of the phase screen is assumed to be a stationary Gaussian random field. For more general simulation approaches for turbulence in random media see direct numerical simulation and large-eddy simulation in chapters 8 and 9 of [10]. In addition for other classical numerical simulation methods of phase screens see [7] and the references within.

Most previous work on the study of phase screens has been on uncorrelated phase screens. If the distance between phase screens is sufficiently small then the screens are guaranteed to be correlated. Intuitively it is clear that the correlation between phase screens increases as they are placed closer to each other. It is assumed that in the space between phase screens, the phase does not change. For examples of results based on uncorrelated phase screens see for example [5,17,18].

Recently some sources have considered correlated phase screens. Naeh and Katzir in [8] proposed the Sparse Spectrum Harmonic Augmentation (SSHA) method, which simulates perfectly correlated

☆ Supported partially by Office of Naval Research's (ONR) Atmospheric Propagation Sciences for High Energy Lasers (APSHELS).
* Corresponding author at: Department of Engineering Physics, Center for Directed Energy, Wright-Patterson AFB, Dayton, OH 45433, USA.

http://dx.doi.org/10.1016/j.optcom.2017.01.015
Received 25 September 2016; Received in revised form 29 December 2016; Accepted 10 January 2017
Available online 18 January 2017
0030-4018/ Published by Elsevier B.V.

phase screens in an isotropic three-dimensional media. The method compresses three-dimensional refractive index media to two-dimensional phase screens and for its implementation one needs the discrete frequency, amplitude, random phase and vector directions. Also [9] simulated correlated phase screens by calculating the auto-correlation (correlation between two points on the same screen) and cross-correlation (correlation between two points on two different phase screens) of change in phase. In contrast to our approach they do not take into account the Markov property of the phase screens. However, similar to our method they use the Fast Fourier transform to convert delta-correlated random numbers in the spatial domain to the spectral domain by using the relation between a phase screen with its spectrum by the Fourier transform pair,

$$\Phi(\mathbf{k}) = \int p(\mathbf{r}) e^{-2\pi i \mathbf{r}\cdot\mathbf{k}} d\mathbf{r} \tag{1a}$$

$$p(\mathbf{r}) = \int \Phi(\mathbf{k}) e^{2\pi i \mathbf{k}\cdot\mathbf{r}} d\mathbf{k} \tag{1b}$$

where $\Phi(\mathbf{k})$ is the spectrum of the phase fluctuations and $p(\mathbf{r})$ is the phase screen at $\mathbf{r} = (x, y)$. Their simulated phase screens demonstrate that the larger pockets of air show more correlation, which is also what we have observed in our simulated phase screens. For the simulation of correlated phase screens see also [19]. Here we consider correlated phase screens based on temperature, where the distance between the screens is measured as a fraction of the integral length scale and is on the order of meters.

This article is organized as follows. Section 2 describes our new approach to Fourier filtering method. The application of this technique to generate correlated phase screens is given in Section 3. In Section 4, we analytically examine the effects of Markov property on estimating temperature at a fixed point on a phase screen along the path, knowing the temperature at this point on the screen before it. Then in Section 5, we provide an algorithm based on the new Fourier filtering method given in Section 2, that can be used to generate phase screens with Markov property. Section 6 provides a description on our numerical results along with our figures illustrating our simulations. We conclude with Section 7 with a summary of our results. All of our findings can be applied to two and three dimensional phase screens. Without loss of generality, we focus on three dimensional screens and note that the results can be easily modified to two dimensional screens without requiring changes to the techniques.

2. Fourier filtering method

In this section we present a new approach to the Fourier filtering method. Suppose we have a real-valued stationary isotropic Gaussian random field $X(\mathbf{x})$ with $\mathbf{x} = (x, y, z)$ and domain being a three dimensional finite lattice, denoted as $\mathcal{D}$. In addition, suppose we are given that for all $\mathbf{x} \in \mathcal{D}$,

$$\mathbb{E}(X) = 0, \tag{2a}$$

$$\mathbb{E}(X^2) = \sigma^2 < \infty, \tag{2b}$$

with autocorrelation,

$$f(|\mathbf{r}|) = \mathbb{E}(X(\mathbf{x})X(\mathbf{x}')) = \mathbb{E}(X(\mathbf{x})X(\mathbf{x}-\mathbf{r})) \tag{2c}$$

where $\mathbf{x}$ and $\mathbf{x}'$ are two position vectors and $|\mathbf{r}| = |\mathbf{x} - \mathbf{x}'|$ is the distance between them. Autocorrelation is a function of $|\mathbf{r}|$, which we assume to be continuous and positive definite so that by Bochner's theorem (see Pg. 303 of [13]), its Fourier transform, $\hat{f}$, is real and positive.

By the zero mean assumption on X, we have, for a vector, $\mathbf{k}$ in the Fourier space,

$$0 = \mathcal{F}[\mathbb{E}(X)](\mathbf{k}) = \mathbb{E}(\mathcal{F}[X](\mathbf{k})) = \mathbb{E}(\widehat{X}(\mathbf{k})). \tag{3}$$

As an application of the convolution theorem for Fourier transforms we have,

$$\begin{aligned}\int_{\mathcal{D}} \hat{f}(|\mathbf{k}|)d\mathbf{x} &= \mathcal{F}\left(\mathbb{E}\left(\int_{\mathcal{D}} X(\mathbf{x})X(\mathbf{x}-\mathbf{r})d\mathbf{x}\right)\right)\\ &= \mathbb{E}\left(\mathcal{F}\left(\int_{\mathcal{D}} X(\mathbf{x})X(\mathbf{x}-\mathbf{r})d\mathbf{x}\right)\right) = \mathbb{E}(\widehat{X}(\mathbf{k})\cdot\overline{\widehat{X}}(\mathbf{k}))\end{aligned} \tag{4}$$

so that,

$$\hat{f}(|\mathbf{k}|) = \frac{\mathbb{E}(\widehat{X}(\mathbf{k})\cdot\overline{\widehat{X}}(\mathbf{k}))}{\int_{\mathcal{D}} d\mathbf{x}} \tag{5}$$

where we have used the Fubini's theorem repeatedly since by applying Cauchy–Schwartz inequality, we have $X(\mathbf{x})X(\mathbf{x}-\mathbf{r}) \in L^1$. For the simplicity of notation, we take into account the finite assumption on $\mathcal{D}$ and let $\mu(\mathcal{D}) := \int_{\mathcal{D}} d\mathbf{x} < \infty$ be the Lebesgue measure of $\mathcal{D}$.

Since $X(\mathbf{x})$ is a real-valued Gaussian random field, then its Fourier transform, $\widehat{X}(\mathbf{k}) := U(\mathbf{k}) + iV(\mathbf{k})$, is also Gaussian and by Cramer's theorem (see Theorem 6.19 of [3]), U and V are independent Gaussian random variables. Let $U(\mathbf{k}) \sim N(\mu_1(\mathbf{k}), \sigma_1^2(\mathbf{k}))$ and $V(\mathbf{k}) \sim N(\mu_2(\mathbf{k}), \sigma_2^2(\mathbf{k}))$. Since by assumption, X has mean zero and variance, $\sigma^2 < \infty$ then,

$$\mathbb{E}(\widehat{X}(\mathbf{k})) = 0, \tag{6a}$$

$$\mu_1(\mathbf{k}) = \mu_2(\mathbf{k}) = 0. \tag{6b}$$

Let $\tilde{\sigma}^2(\mathbf{k})$ denote the variance of $\widehat{X}(\mathbf{k})$ then, we have, using the independence property of $U(\mathbf{k})$ and $V(\mathbf{k})$,

$$\begin{aligned}\mathbb{E}(\widehat{X}(\mathbf{k})\cdot\overline{\widehat{X}}(\mathbf{k})) = \mathbb{E}(U^2(\mathbf{k}) + V^2(\mathbf{k})) &= \mathbb{E}(U(\mathbf{k}))^2 + \mathbb{E}(V(\mathbf{k}))^2 + \sigma_1^2(\mathbf{k})\\ &+ \sigma_2^2(\mathbf{k}) = \mu_1^2(\mathbf{k}) + \mu_2^2(\mathbf{k}) + \tilde{\sigma}^2(\mathbf{k}) = \tilde{\sigma}^2(\mathbf{k})\end{aligned} \tag{7}$$

so by Eq. (5) we have,

$$\mu(\mathcal{D})\hat{f}(|\mathbf{k}|) = \mathbb{E}(\widehat{X}(\mathbf{k})\cdot\overline{\widehat{X}}(\mathbf{k})) = \tilde{\sigma}^2(\mathbf{k}) \tag{8}$$

giving, $\widehat{X}(\mathbf{k}) \sim N(0, \mu((D))\hat{f}(|\mathbf{k}|)) + iN(0, \mu(\mathcal{D})\hat{f}(|\mathbf{k}|))$ and f being positive definite makes $\hat{f}$ real and positive assuring that the variance is real and positive.

Now assume we are given a real-valued Gaussian random field, $X(\mathbf{x})$ with the same properties as in the previous case with the exception that $\mathbb{E}(X(\mathbf{x})) = g(\mathbf{x})$, where g is a given real function. With the same equalities as in (3), we obtain,

$$\mathbb{E}(\widehat{X}(\mathbf{k})) = \hat{g}(\mathbf{k}). \tag{9}$$

Using the Gaussian distribution for the Fourier transform of X as in the previous case, we have $\hat{g}(\mathbf{k}) = \mu_1(\mathbf{k}) + i\mu_2(\mathbf{k})$ and by (5) and similar to (7),

$$\mu(\mathcal{D})\hat{f}(|\mathbf{k}|) = \mathbb{E}(\widehat{X}(\mathbf{k})\cdot\overline{\widehat{X}}(\mathbf{k})) = \mu_1^2(\mathbf{k}) + \mu_2^2(\mathbf{k}) + \tilde{\sigma}^2(\mathbf{k}) = |\hat{g}(\mathbf{k})|^2 + \tilde{\sigma}^2(\mathbf{k}) \tag{10}$$

so that

$$\begin{aligned}\widehat{X}(\mathbf{k}) &\sim N(Re(\hat{g}(\mathbf{k})), \mu(\mathcal{D})\hat{f}(|\mathbf{k}|) - |\hat{g}(\mathbf{k})|^2)\\ &+ iN(Im(\hat{g}(\mathbf{k})), \mu(\mathcal{D})\hat{f}(|\mathbf{k}|) - |\hat{g}(\mathbf{k})|^2)\end{aligned}$$

To confirm the positivity of $\mu(\mathcal{D})\hat{f}(|\mathbf{k}|) - |\hat{g}(\mathbf{k})|^2$, observe that,

$$\begin{aligned}|\hat{g}(\mathbf{k})|^2 = |\mathbb{E}(\widehat{X}(\mathbf{k}))|^2 = |\mathbb{E}(U(\mathbf{k})) + i\mathbb{E}(V(\mathbf{k}))|^2 &= \mathbb{E}(U(\mathbf{k}))^2 + \mathbb{E}(V(\mathbf{k}))^2\\ \le \mathbb{E}(U^2(\mathbf{k})) + \mathbb{E}(V^2(\mathbf{k})) = \mathbb{E}(\widehat{X}(\mathbf{k})\cdot\overline{\widehat{X}}(\mathbf{k})) &= \mu(\mathcal{D})\hat{f}(|\mathbf{k}|)\end{aligned} \tag{11}$$

thus, limiting the choice of g.

3. Generation of temperature values on a fixed phase screen

We apply the Fourier filtering method presented in the previous section to generate phase screens in a three dimensional temperature field, denoted as $\mathcal{D}$. We assume the phase screens to be correlated based on temperature and the distance between them to be the same. Let $\mathbf{x}' = (x', y')$ be a fixed point on phase screen at z and $\mathbf{x} = (x, y)$ be

any other point on this screen. Furthermore, denote the temperature at position $\mathbf{x}$ in the screen at point z as $T(\mathbf{x}, z)$. According to Section 2, suppose we are given,

$$\mathbb{E}(T(\mathbf{x}', z)) = g(\mathbf{x}', z) \tag{12a}$$

$$\mathbb{E}(T(\mathbf{x}', z)^2) - g(\mathbf{x}', z)^2 = \sigma^2 < \infty \tag{12b}$$

and that the autocorrelation is provided as

$$\mathbb{E}(T(\mathbf{x}, z)T(\mathbf{x}', z')) = f(|\mathbf{r}|) = f(\sqrt{(x-x')^2 + (y-y')^2 + (z-z')^2}). \tag{13}$$

We use the following algorithm to generate a random temperature field.

1. Take the Fourier transform of the autocorrelation:

$$\mathcal{F}[\mathbb{E}(T(\mathbf{x}, z)T(\mathbf{x}', z'))] = \mathcal{F}[f(|\mathbf{r}|)] = \widehat{f}(|\mathbf{k}|) \tag{14}$$

2. Let

$$\widehat{T}(\mathbf{k}) = U(\mathbf{k}) + iV(\mathbf{k}) \tag{15}$$

where

$$U \sim N(Re(\widehat{g}(\mathbf{k})), \max\{\mu(\mathcal{D})\widehat{f}(|\mathbf{k}|) - |\widehat{g}(\mathbf{k})|^2, 0\}), \tag{16a}$$

$$V \sim N(Im(\widehat{g}(\mathbf{k})), \max\{\mu(\mathcal{D})\widehat{f}(|\mathbf{k}|) - |\widehat{g}(\mathbf{k})|^2, 0\}). \tag{16b}$$

3. A random temperature field with the given autocorrelation can be generated by,

$$T(\mathbf{x}, z) = \mathcal{F}^{-1}[\widehat{T}(\mathbf{k})] \tag{17}$$

Hence, knowing the autocorrelation between two points and the average value, we can generate values for the temperature at any point in $\mathcal{D}$.

4. Correlated phase screens with Markov property

In this section we investigate the correlation of phase screens based on temperature, by examining it analytically. The screens can be thought of as sheets in the two dimensional case and rectangular boxes having volume in the three dimensional case. We assume the screens to have equal size arranged with different distance between them in the z direction. Based on experimental data, the temperature at each point on a phase screen is Gaussian with possibly nonzero mean. We assume that the screens have the Markov property so that the temperature at a screen only depends on the known temperature of the latest phase screen before it.

Let $\mathbf{x}'$ be a fixed point on the phase screen at z_i. Given temperature $T(\mathbf{x}', z_i)$, we estimate the temperature at the fixed point, $\mathbf{x}'$, on a screen at z_{i+1}, which is further along the z direction by distance $|z_{i+1} - z_i|$. To match the setting of the Fourier filtering method, introduced in the previous section, we assume that we are given,

$$\mathbb{E}(T(\mathbf{x}', z_i)T(\mathbf{x}', z_{i+1})) = f(|z_{i+1} - z_i|), \tag{18}$$

where as required by the method, f is a continuous, positive definite real function. We determine

$$\begin{aligned} f(|z_{i+1} - z_i|) &= \mathbb{E}(T(\mathbf{x}', z_i)T(\mathbf{x}', z_{i+1})) \\ &= \mathbb{E}(\mathbb{E}(T(\mathbf{x}', z_i)T(\mathbf{x}', z_{i+1})|T(\mathbf{x}', z_0) = t_{z_0}, \ldots, T(\mathbf{x}', z_i) = t_{z_i})) \\ &= \mathbb{E}(T(\mathbf{x}', z_i)\mathbb{E}(T(\mathbf{x}', z_{i+1})|T(\mathbf{x}', z_0) = t_{z_0}, \ldots, T(\mathbf{x}', z_i) = t_{z_i})) \\ &= \mathbb{E}(T(\mathbf{x}', z_i)\mathbb{E}(T(\mathbf{x}', z_{i+1})|T(\mathbf{x}', z_i) = t_{z_i})) \end{aligned} \tag{19}$$

where t_{z_i} is the temperature at the point $\mathbf{x}'$ on the screen at z_i and the Markov property has been applied. Since $\mathbb{E}(T(\mathbf{x}', z_{i+1})|T(\mathbf{x}', z_i) = t_{z_i}) = h(T(\mathbf{x}', z_i))$ for some real function, h, we obtain

$$f(|z_{i+1} - z_i|) = \mathbb{E}(T(\mathbf{x}', z_i)T(\mathbf{x}', z_{i+1})) = \mathbb{E}(T(\mathbf{x}', z_i)h(T(\mathbf{x}', z_i))) \tag{20}$$

Now based on the given information, the only candidate for $h(T(\mathbf{x}', z_i))$, that would not require more assumptions on the temperature, is $h(T(\mathbf{x}', z_i)) = KT(\mathbf{x}', z_i)$ where K is a positive constant. Using Eq. (20), $K = f(|z_{i+1} - z_i|)/\mathbb{E}(T(\mathbf{x}', z_i)^2)$, thus, we obtain

$$\mathbb{E}(T(\mathbf{x}', z_{i+1})|T(\mathbf{x}', z_i) = t_{z_i}) = h(T(\mathbf{x}', z_i)) = \frac{f(|z_{i+1} - z_i|)}{f(0)}T(\mathbf{x}', z_i) \tag{21}$$

where $f(0) = \mathbb{E}(T(\mathbf{x}', z_i)^2) > 0$ and by the positive definite property of f, $|f(|z_{i+1} - z_i|)| < f(0)$.

If the distance between each phase screen is constant we can use the Markov property to find the correlation between all screens. We let this equal distance be denoted by an integer $\alpha > 1$. To determine the correlation between phase screens at z_i and $z_{i+\alpha}$ we have,

$$\begin{aligned} &\mathbb{E}(T(\mathbf{x}', z_i)T(\mathbf{x}', z_{i+\alpha})) \\ &= \mathbb{E}(T(\mathbf{x}', z_i)\mathbb{E}(T(\mathbf{x}', z_{i+\alpha})|T(\mathbf{x}', z_{i+\alpha-1}) = t_{z_{i+\alpha-1}})) \\ &= \mathbb{E}(T(\mathbf{x}', z_i)h(T(\mathbf{x}', z_{i+\alpha-1}))). \end{aligned} \tag{22}$$

Similar to above we pick $h(T(\mathbf{x}', z_{i+\alpha-1})) = KT(\mathbf{x}', z_{i+\alpha-1})$ arriving at,

$$\mathbb{E}(T(\mathbf{x}', z_i)T(\mathbf{x}', z_{i+\alpha})) = K\mathbb{E}(T(\mathbf{x}', z_i)T(\mathbf{x}', z_{i+\alpha-1})). \tag{23}$$

Therefore, repeating this process α times yields

$$\mathbb{E}(T(\mathbf{x}', z_i)T(\mathbf{x}', z_{i+\alpha})) = K^\alpha\mathbb{E}(T(\mathbf{x}', z_i)^2) \tag{24}$$

which confirms the exponential behavior we have observed in Fig. 1.

5. Generation of correlated phase screens with Markov property

Here we generate arbitrary spaced phase screens having Markov property and apply our results from Section 4. Suppose phase screens are not necessarily equally spaced. Suppose we have (12a) and (12b) and in addition, assume we are given the autocorrelation function and the correlation between phase screens at z_i and z_{i-1} as,

$$\mathbb{E}(T(\mathbf{x}, z_i)T(\mathbf{x}', z_i)) = f(|\mathbf{x} - \mathbf{x}'|), \tag{25a}$$

$$h(T(\mathbf{x}', z_i)) = \mathbb{E}(T(\mathbf{x}', z_i)|T(\mathbf{x}', z_{i-1}) = t_{z_{i-1}}) = \frac{f(|z_i - z_{i-1}|)}{f(0)}T(\mathbf{x}', z_{i-1}). \tag{25b}$$

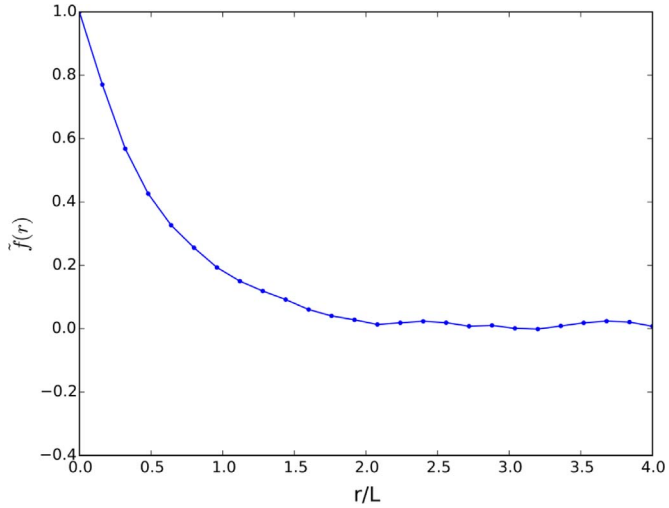

Fig. 1. Numerically calculated correlation between the phase screen as a function of integral length scale.

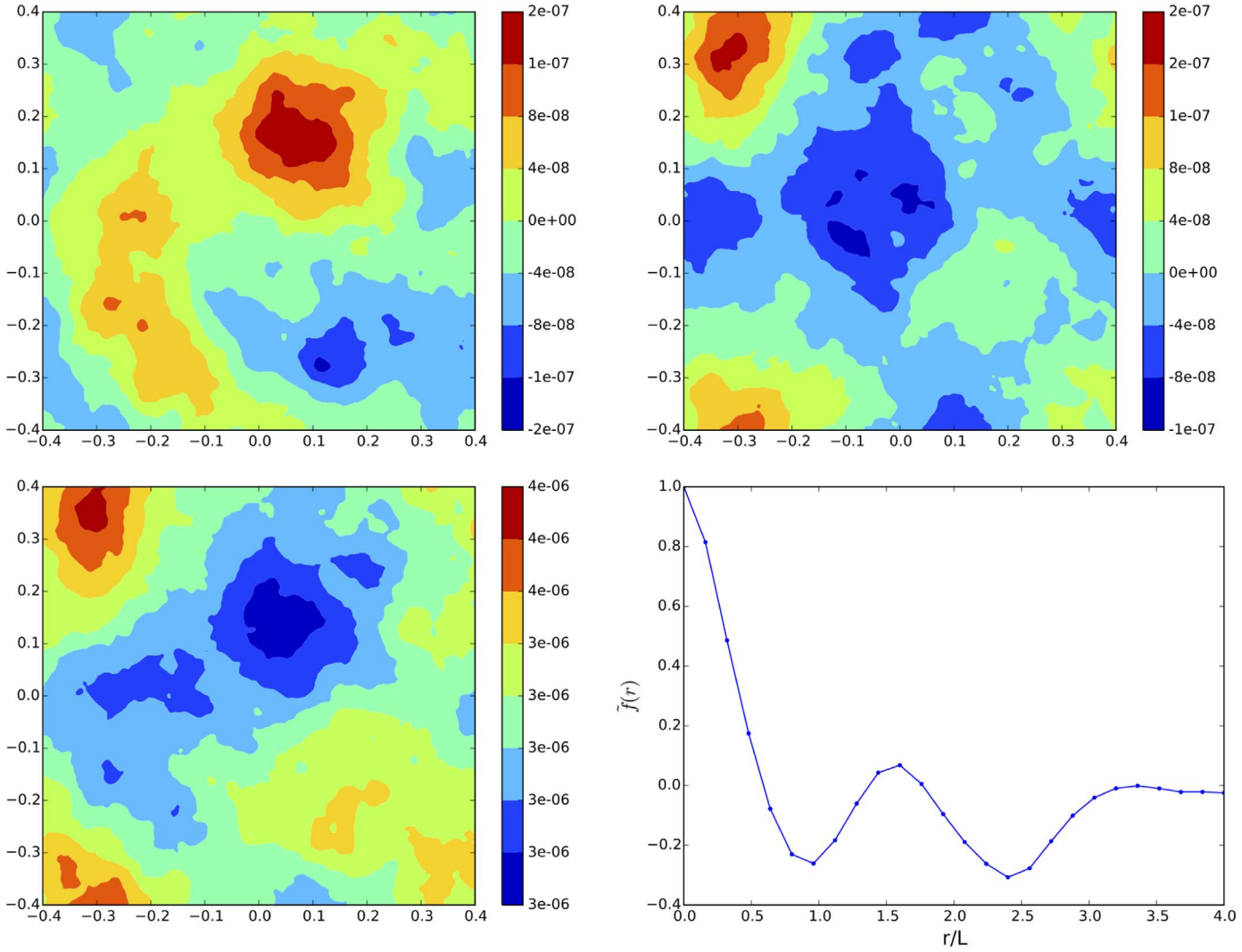

Fig. 2. Slices of temperature field generated by the algorithm described in Section 3. No wrapping mitigation techniques was utilized. Top left is the first slice. Top right is the second slice. Bottom left is the difference between the two slices. Bottom right is the numerically calculated correlation between the temperature slices as a function of integral length scale.

To generate correlated phase screens in this setting we follow the steps below.

1. Take the Fourier transform of the autocorrelation function:

$$\mathcal{F}[\mathbb{E}(T(\mathbf{x}, z_i)T(\mathbf{x}', z_i))] = \mathcal{F}[f(|\mathbf{r}|)] = \widehat{f}(|\mathbf{k}|) \tag{26}$$

2. Make the phase screen at z_i be dependent on the previous phase screen, z_i:

$$\widehat{h}(\mathbf{k}, z_i) = \begin{cases} g(\mathbf{k}, z_0), & \text{if } i = 0, \\ g(\mathbf{k}, z_i) + \dfrac{f(|z_i - z_{i-1}|)}{f(0)}\widehat{T}(\mathbf{x}', z_{i-1}), & \text{else.} \end{cases} \tag{27}$$

Note that i=0 indicates the first phase screen.

3. Let,

$$\widehat{T}(\mathbf{k}, z_i) = U(\mathbf{k}) + iV(\mathbf{k}), \tag{28}$$

where

$$U \sim N(Re(\widehat{h}(\mathbf{k}, z_i)), \max\{\mu(\mathcal{D})\widehat{f}(|\mathbf{k}|) - |\widehat{h}(\mathbf{k}, z_i)|^2, 0\}), \tag{29a}$$

$$V \sim N(Im(\widehat{h}(\mathbf{k}, z_i)), \max\{\mu(\mathcal{D})\widehat{f}(|\mathbf{k}|) - |\widehat{h}(\mathbf{k}, z_i)|^2, 0\}). \tag{29b}$$

4. The phase screen at position z_i is obtained by,

$$\mathcal{F}^{-1}(\widehat{T}(\mathbf{k}, z_i)) = T(\mathbf{x}, z_i). \tag{30}$$

5. Repeat steps 2–4 until all phase screens have been generated.

6. Numerical results

We now provide phase screens that we have simulated using the method described. Figs. 2 and 3 illustrate phase screens generated by algorithms presented by Sections 3 and 5, respectively, using the three dimensional spectrum given by [10, p. 232],

$$E(\kappa) = \oint_{\kappa} |\widehat{f}(k_1, k_2, k_3)|^2 \kappa^2 \sin\phi d\phi d\theta = \left(\frac{\kappa L}{\sqrt{(\kappa L)^2 + c_L}}\right)^{5/3+p_0} \kappa^{-5/3} e^{-\beta\kappa l_K}, \tag{31}$$

where $\kappa = \sqrt{k_1^2 + k_2^2 + k_3^2}$. The above parameters determine the temperature spectrum and are set as,

- L: integral length scale, here 50 m,
- l_K: Kolmogorov micro-scale, here 1 mm,
- c_L: a positive constant, depending on integral length scale, here 6.78,

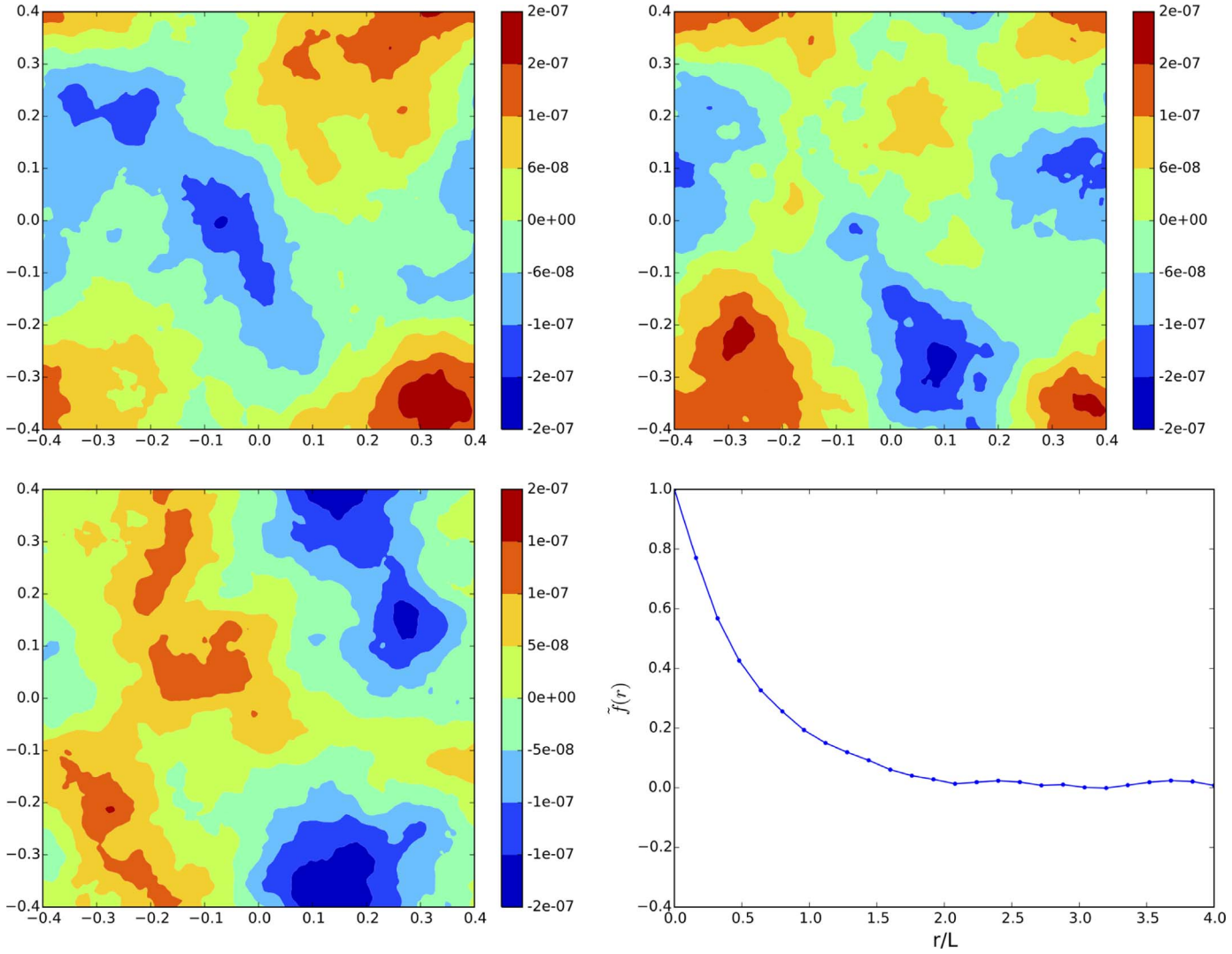

Fig. 3. Sequence of phase screens described in Section 5. Phase screens using the spectrum defined in Eq. (31). No wrapping mitigation techniques was utilized. Top left is the first phase screen. Top right is the second phase screen. Bottom left is the difference between the phase screens. Bottom right is the numerically calculated correlation between the phase screens as a function of integral length scale.

- p_0: a positive constant, determining the power of the three dimensional energy function spectrum and as $\kappa \to 0$, $p_0 = 4$,
- $\beta = 5.2$
- $c_\eta = 0$

No wrapping mitigation techniques were utilized. In Figs. 2 and 3, the phase screens on the top left represent the screen at point z_i and the one on the top right is the screen at z_{i+1}. The difference between the screens is in bottom left. Correlation between the slices is clear and an estimate for this correlation is given by,

$$\widetilde{f}(r) = \frac{1}{N_1 N_2 N_3} \sum_{i=0}^{N_1} \sum_{j=0}^{N_2} \sum_{k=0}^{N_3} T(x_i, y_j, z_k) T(x_i, y_z, z_k + r), \tag{32}$$

where N_1, N_2 and N_3 represent the number of grid points in x, y and z, respectively. The estimated correlation between slices are plotted against the integral length scale and are shown in the bottom right of Figs. 2 and 3.

7. Results

In this article we described a technique for generating temperature fields with a known correlation function. The traditional method is to create a correlation matrix and factorize the matrix using the Cholesky factorization. The algorithm described here only uses the Fast Fourier Transform and is computationally faster and requires less memory. We also presented a method for generating correlated phase screens based on the Markov property. The new method can also generate random fields with non-zero and spatial varying mean.

Acknowledgements

We would like to thank Dr. Steven Fiorino for his support as the director of the Center for Directed Energy (CDE) at the Air Force Institute of Technology (AFIT). Dr. Fiorino and team members of CDE, such as Dr. Santasri Basu and Dr. Jack McCrae offered helpful conversations and insight into the physics of laser related problems and the one described here. CDE provided us valuable resources and dynamic research atmosphere to conduct our research. We also like to thank the editor and an anonymous referee for their comments and insights. The first author is thankful to Oak Ridge Institute for Science and Education (ORISE) and the second author is grateful to National Research Council (NRC) for making this research possible by serving as an interagency between the U.S. Department of Energy and AFIT and effectively taking care of its administrative tasks.

References

[1] A. Zardecki, C. Delisle, Higher order statistics of light scattered by a random phase screen, Opt. Acta 24 (3) (1977) 241–259.
[2] L. Andrews, R. Phillips, Laser Beam Propagation Through Random Media, The International Society for Optical Engineering, SPIE Press, Bellingham, Washington, USA. 2005.
[3] H. Cramer, Random Variables and Probability Distributions, At the University Press, Cambridge, 1970.
[4] A. Dieker, M. Mandjes, On spectral simulation of fractional Brownian motion, Probab. Eng. Inform. Sci. 17 (3) (2003) 417–434.
[5] A. Dipankar, P. Sagaut, A new phase-screen method for electromagnetic wave propagation in turbulent flows using large-eddy simulation, J. Comput. Phys. 228 (20) (2009) 7729–7741.
[6] C. Dietrich, G. Newsam, Fast and exact simulation of stationary Gaussian processes through circulant embedding of the covariance matrix, SIAM J. Sci. Comput. 18 (4) (1997) 1088–1107.
[7] R. Lane, A. Glindemann, J. Dainty, Simulation of a Kolmogorov phase screen, Waves Random Media 2 (3) (1992) 209–224.
[8] I. Naeh, A. Katzir, Perfectly correlated phase screen realization using sparse spectrum harmonic augmentation, Appl. Opt. 53 (27) (2014) 6168–6174.
[9] P. Paramonov, A. Vorontsov, V. Kunitsyn, A three-dimensional refractive index model for simulation of optical wave propagation in atmospheric turbulence, Waves Random Complex Media 25 (4) (2015) 556–575.
[10] S. Pope, Turbulent Flows, Cambridge University Press, Cambridge, United Kingdom, 2000.
[11] M. Roggemann, B. Welsh, Imaging through turbulence, in: Laser and Optical Science and Technology Series, CRC Press, Boca Raton, Florida, USA, 1996.
[12] F. Roux, The Lindblad equation for the decay of entanglement due to atmospheric scintillation, J. Phys. A 47 (19) (2014) 15–pp.
[13] W. Rudin, Functional analysis, second edition, International Series in Pure and Applied Mathematics, 1991.
[14] J. Schmidt, Numerical Simulation of Optical Wave Propagation with Examples in Matlab, SPIE Press, New York, USA, 2010.
[15] V. Schmidt, Stochastic geometry, spatial statistics and random fields, Lect. Notes Math. 2120 (2014).
[16] J. Strohbehn, Laser Beam Propagation in the Atmosphere, Topics in Applied Physics, vol. 25, Springer, New York, 1978.
[17] B. Uscinski, Analytical solution of the fourth-moment equation and interpretation as a set of phase screens, J. Opt. Soc. Am. A 2 (12) (1985) 2077–2091.
[18] A. Vorontsov, P. Paramonov, M. Valley, M. Vorontsov, Generation of infinitely long phase screens for modeling of optical wave propagation in atmospheric turbulence, Waves Random Complex Media 18 (1) (2008) 91–108.
[19] B. Welsh, Fourier-series-based atmospheric phase screen generator for simulating anisoplanatic geometries and temporal evolution, Proc. SPIE 3125 (1997).
[20] A. Wild, R. Hobbs, L. Frenje, Modelling complex media: an introduction to the phase-screen method, Phys. Earth Planet. Inter. 120 (3) (2000) 219–225.
[21] X. Xiao, D. Voelz, Wave optics simulation approach for partial spatially coherent beams, Opt. Exp. 14 (16) (2006) 6986–6992.
[22] Z. Yin, New methods for simulation of fractional Brownian motion, J. Comput. Phys. 127 (1) (1996) 66–72.